
On the Nonlinear Transfer of Energy in the Peak of a Gravity-Wave Spectrum. II

Author(s): M. J. H. Fox

Source: *Proceedings of the Royal Society of London. Series A, Mathematical and Physical Sciences*, Vol. 348, No. 1655 (Apr. 6, 1976), pp. 467-483

Published by: The Royal Society

Stable URL: <http://www.jstor.org/stable/79073>

Accessed: 06/01/2009 05:13

Your use of the JSTOR archive indicates your acceptance of JSTOR's Terms and Conditions of Use, available at <http://www.jstor.org/page/info/about/policies/terms.jsp>. JSTOR's Terms and Conditions of Use provides, in part, that unless you have obtained prior permission, you may not download an entire issue of a journal or multiple copies of articles, and you may use content in the JSTOR archive only for your personal, non-commercial use.

Please contact the publisher regarding any further use of this work. Publisher contact information may be obtained at <http://www.jstor.org/action/showPublisher?publisherCode=rsl>.

Each copy of any part of a JSTOR transmission must contain the same copyright notice that appears on the screen or printed page of such transmission.

JSTOR is a not-for-profit organization founded in 1995 to build trusted digital archives for scholarship. We work with the scholarly community to preserve their work and the materials they rely upon, and to build a common research platform that promotes the discovery and use of these resources. For more information about JSTOR, please contact support@jstor.org.



The Royal Society is collaborating with JSTOR to digitize, preserve and extend access to *Proceedings of the Royal Society of London. Series A, Mathematical and Physical Sciences*.

On the nonlinear transfer of energy in the peak of a gravity-wave spectrum. II

BY M. J. H. FOX

*Department of Applied Mathematics and Theoretical Physics,
Silver Street, Cambridge*

(Communicated by M. S. Longuet-Higgins, F.R.S. – Received 28 July 1975)

This paper presents the first accurate calculations of the nonlinear transfer of energy within a continuous spectrum of water waves. The spectrum is assumed to be narrow, that is, the wave energy is initially concentrated near one particular wavenumber, and use is made of the transfer equation derived previously in part I (Longuet-Higgins 1975) for this case. It is shown that when the spectrum is describable as a sum of normal distributions, then the sixfold multiple integral can be reduced to a single integration. Hence the accurate evaluation of the energy transfer (as a function of the two dimensional wavenumber) becomes practicable.

For a symmetric normal spectrum it is found that the transfer function generally has the form of a clover-leaf, with four maxima lying in the characteristic directions $d\lambda = \pm \sqrt{2}d\mu$, as seen from the peak. These are separated by troughs of negative transfer lying in the axial directions $d\lambda = 0, d\mu = 0$. For a typically asymmetric spectrum, one of the negative troughs may be filled in, so that the transfer function more closely resembles a butterfly. An interpretation is given in terms of the balance of terms in the transfer equation.

The (one dimensional) transfer function for the frequency-spectrum can be found by integration of the two dimensional transfer function. Typically it has a pronounced minimum near the peak frequency, indicating strong negative transfer there, and two weaker maxima, one on each side. For asymmetric spectra, the maximum transfer is greater on the steeper face of the spectrum, usually on the low-frequency side. A comparison with the rough calculations of Sell & Hasselmann (1972) for the JONSWAP R3C spectrum shows good agreement.

1. INTRODUCTION

This paper continues the calculation and interpretation of the nonlinear energy transfer in a continuous spectrum of deep-water waves, which was begun in a previous paper (part I, Longuet-Higgins 1975). That paper considered an ideal case in which the energy was all concentrated in the neighbourhood of the spectral peak. By making use of an evolution equation due to Davey & Stewartson (1974), a simplified expression was found for the energy flux. Hence it was shown that the energy flowed away from the spectral peak in certain characteristic directions,

and that for a normally-shaped peak the rate of change at the summit was negative.

The detailed calculation of the energy flux to all parts of the spectrum was seen to depend on a multiple integral which in general must be evaluated numerically. Because of the computing time involved a satisfactory degree of accuracy is hard to achieve. However, in the particular case of the normal (bell-shaped) peak we shall show that the multiple integral can actually be reduced to a single integral. This then allows us to evaluate the energy transfer accurately at all points of the wavenumber plane, and to draw smooth contours of energy flux, an achievement not found possible previously (Sell & Hasselmann 1972; Hasselmann *et al.* 1973).

It then becomes clear (§4) that the initial flux has the form of a four-leafed clover (see, for example, figure 2*a*), the four maxima lying near the characteristic lines as predicted earlier. The flux of energy as a function of frequency alone can also be found accurately, by a further integration.

In §5 we extend the technique to the case when the spectrum is representable as the sum of two or more different normal distributions. Hence we can discuss also the effects of asymmetry in the energy spectrum.

Lastly, in §6 we calculate the energy transfer in a typical sea state on the assumption that the directional spectrum can in fact be represented as the sum of three bell-shaped functions; and we compare the results with the previous calculations by Hasselmann *et al.* (1973).

2. BASIC EQUATIONS

The definitions, assumptions and notation will be the same as in part I (Longuet-Higgins 1975). It was there shown that the rate of change of the action-density $N(\boldsymbol{\kappa})$ at wave-number $\boldsymbol{\kappa}$ near the spectral peak is given by an expression of the form

$$\frac{\partial N_1}{\partial \tau} = 4\pi \int \dots \int [(N_1 + N_2) N_3 N_4 - (N_3 + N_4) N_1 N_2] \times \delta(\boldsymbol{\kappa}_1 + \boldsymbol{\kappa}_2 - \boldsymbol{\kappa}_3 - \boldsymbol{\kappa}_4) \delta(\omega_1 + \omega_2 - \omega_3 - \omega_4) d\boldsymbol{\kappa}_2 d\boldsymbol{\kappa}_3 d\boldsymbol{\kappa}_4 \quad (2.1)$$

in non-dimensional units, where $N_i \equiv N(\boldsymbol{\kappa}_i)$ and $\delta(\)$ denotes the Dirac delta function. ω_i and $\boldsymbol{\kappa}_i$ are related by $\omega_i^2 = -\frac{1}{8}(\lambda_i^2 - 2\mu_i^2) + 2M$, where $(\lambda_i, \mu_i) = \boldsymbol{\kappa}_i$ and M is a constant. In part I, appendix B it is shown that this sixfold multiple integral can be reduced in general to the triple integral

$$\frac{\partial N_1}{\partial \tau} = 32\pi \iiint [(N_1 + N_2) N_3 N_4 - (N_3 + N_4) N_1 N_2] \frac{d\alpha d\beta' d\beta''}{|J'J''|}, \quad (2.2)$$

where

$$\left. \begin{aligned} (\lambda', \mu') &= \boldsymbol{\kappa}' = \frac{1}{2}(\boldsymbol{\kappa}_2 - \boldsymbol{\kappa}_1), \\ (\lambda'', \mu'') &= \boldsymbol{\kappa}'' = \frac{1}{2}(\boldsymbol{\kappa}_4 - \boldsymbol{\kappa}_3), \end{aligned} \right\} \quad (2.3)$$

(see figure 3 of part I),

$$\alpha = (\lambda'^2 - 2\mu'^2) = (\lambda''^2 - 2\mu''^2), \quad (2.4)$$

β' and β'' are some other functions of (λ', μ') and (λ'', μ'') respectively, and

$$J' = \frac{\partial(\alpha, \beta')}{\partial(\lambda', \mu')}, \quad J'' = \frac{\partial(\alpha, \beta'')}{\partial(\lambda'', \mu'')} \tag{2.5}$$

We shall find it convenient to choose

$$\left. \begin{aligned} \beta' &= \lambda' + \sqrt{2\mu'}, \\ \beta'' &= \lambda'' + \sqrt{2\mu''}, \end{aligned} \right\} \tag{2.6}$$

so that

$$J' = \sqrt{8\beta'}, \quad J'' = \sqrt{8\beta''} \tag{2.7}$$

Also

$$\lambda' = \frac{1}{2} \left(\beta' + \frac{\alpha}{\beta'} \right), \quad \mu' = \frac{1}{\sqrt{8}} \left(\beta' - \frac{\alpha}{\beta'} \right), \tag{2.8}$$

and similarly for λ'', μ'' . In the (λ', μ') -plane, the coordinate curves $\alpha = \text{constant}$ are hyperbolae, while the curves $\beta = \text{constant}$ are parallel straight lines (see figure 1). Similarly for (λ'', μ'') .

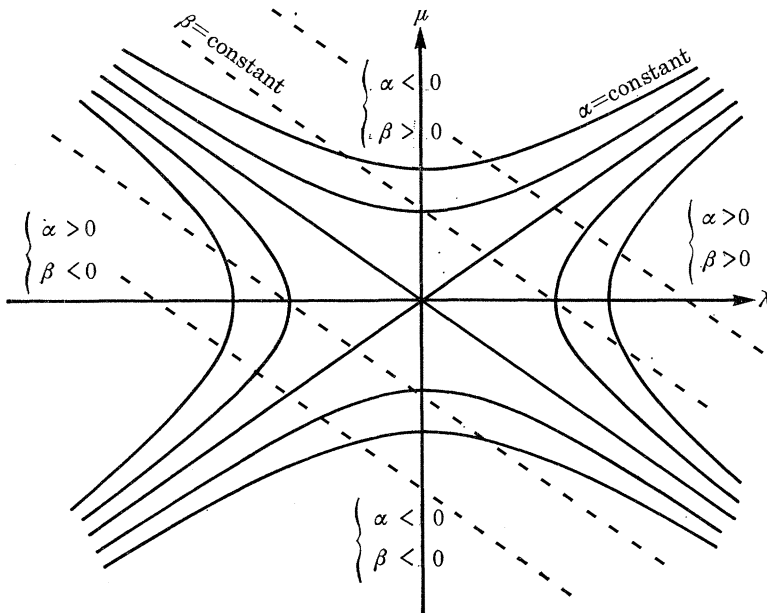


FIGURE 1. Coordinate curves of α and β' in the (λ', μ') -plane.

3. A SYMMETRIC NORMAL SPECTRUM

Suppose initially that the action density has the normal form

$$N(\kappa) = R \exp \left(-\frac{1}{2} P \lambda^2 - Q \mu^2 \right), \tag{3.1}$$

where P, Q and R are positive constants (see part I, §9). Then on substitution in (2.2) we obtain

$$\partial N / \partial \tau = I_1 + I_2 + I_3 + I_4,$$

where

$$I_1 = 4\pi R^3 \iiint \exp \left[-\frac{1}{2}P\{\lambda^2 + (\lambda + \lambda' - \lambda'')^2 + (\lambda + \lambda' + \lambda'')^2\} \right. \\ \left. - Q\{\mu^2 + (\mu + \mu' - \mu'')^2 + (\mu + \mu' + \mu'')^2\} \right] \frac{d\alpha d\beta' d\beta''}{|\beta' \beta''|}, \quad (3.2)$$

and I_2, I_3, I_4 denote three similar expressions. Substitution from (2.8) gives

$$I_1 = 4\pi R^3 \exp \left(-\frac{3}{2}P\lambda^2 - 3Q\mu^2 \right) \iiint \exp \left(-A\alpha^2 - B\alpha - C \right) \frac{d\alpha d\beta' d\beta''}{|\beta' \beta''|}, \quad (3.3)$$

where

$$\left. \begin{aligned} A &= \frac{1}{4}(P+Q) \left(\frac{1}{\beta'^2} + \frac{1}{\beta''^2} \right), \\ B &= (P-Q) + (P\lambda - \sqrt{2Q\mu})|\beta'|, \\ C &= \frac{1}{4}(P+Q) (\beta'^2 + \beta''^2) + (P\lambda + \sqrt{2Q\mu})\beta'. \end{aligned} \right\} \quad (3.4)$$

Integration with respect to α from $-\infty$ to ∞ may be carried out immediately to give

$$I_1 = 8\pi^{\frac{3}{2}}R^3 \exp \left(-\frac{3}{2}P\lambda^2 - 3Q\mu^2 \right) \int_{-\infty}^{\infty} \int_{-\infty}^{\infty} \exp \left(-C + \frac{B^2}{4A} \right) \frac{d\beta' d\beta''}{\sqrt{[(P+Q)(\beta'^2 + \beta''^2)]}}. \quad (3.5)$$

The singularity at $\beta' = \beta'' = 0$ is integrable, and on writing

$$\beta' = r \cos \theta, \quad \beta'' = r \sin \theta, \quad (3.6)$$

we have

$$I_1 = 8\pi^{\frac{3}{2}}R^3 \exp \left(-\frac{3}{2}P\lambda^2 - 3Q\mu^2 \right) \int_{-\frac{1}{2}\pi}^{\frac{1}{2}\pi} \int_{-\infty}^{\infty} \exp [-(Ur^2 + Vr + W)] \frac{dr d\theta}{\sqrt{(P+Q)}}, \quad (3.7)$$

where now

$$\left. \begin{aligned} U &= \frac{P+Q}{4} - \frac{(P-Q)^2}{P+Q} \cos^2 \theta \sin^2 \theta, \\ V &= (P\lambda + \sqrt{2Q\mu}) \cos \theta - 2\frac{P-Q}{P+Q} (P\lambda - \sqrt{2Q\mu}) \cos \theta \sin^2 \theta, \\ W &= -\left(\frac{P\lambda - \sqrt{2Q\mu}}{P+Q} \right)^2 \sin^2 \theta. \end{aligned} \right\} \quad (3.8)$$

We may integrate again with respect to r to obtain

$$I_1 = 16\pi^2 R^3 \exp \left(-\frac{3}{2}P\lambda^2 - 3Q\mu^2 \right) \int_{-\frac{1}{2}\pi}^{\frac{1}{2}\pi} \exp \left(-W + \frac{V^2}{4U} \right) \frac{d\theta}{\sqrt{[(P+Q)^2 - (P-Q)^2 \sin^2 2\theta]}}. \quad (3.9)$$

Thus the original sixfold multiple integral has been reduced to the sum of four single integrals, which can be evaluated quickly and accurately.

Finally we note that reversing the sign of θ simply leaves unchanged the first two integrals, and interchanges the third and fourth. Hence altogether

$$\frac{\partial N}{\partial \tau} = 32\pi^2 R^3 \exp \left(-\frac{3}{2}P\lambda^2 - 3Q\mu^2 \right) \int_0^{\frac{1}{2}\pi} \exp \left(-W + \frac{V^2}{4U} \right) \frac{d\theta}{\sqrt{[(P+Q)^2 - (P-Q)^2 \sin^2 2\theta]}} \\ + \text{three similar expressions.} \quad (3.10)$$

4. NUMERICAL RESULTS: THE SYMMETRIC NORMAL SPECTRUM

The integrals in (3.10) were evaluated numerically by Simpson's rule. Convergence was rapid as the number of integration points increased. In every case 21 points gave an estimated accuracy of at least three significant figures. The evaluation of $\partial N/\partial\tau$ at 2000 points in the κ -plane took about 10 s on an IBM 370/165.

As a check it was found, first, that the computed value of $\partial N/\partial\tau$ at the peak $\kappa = (0, 0)$ agreed precisely with the value found in part I, §9 by an independent method (involving the evaluation of a double integral).

Secondly, the three conservation laws

$$\left. \begin{aligned} \int \frac{\partial N}{\partial\tau} d\kappa &= 0, \\ \int \kappa \frac{\partial N}{\partial\tau} d\kappa &= 0, \\ \int (\lambda^2 - 2\mu^2) \frac{\partial N}{\partial\tau} d\kappa &= 0, \end{aligned} \right\} \quad (4.1)$$

representing the constancy of wave action, momentum and energy respectively, were tested by computing each of the corresponding integrals (except for the μ -component of the second relation, which is satisfied by symmetry about the λ -axis). The relations were all found to be satisfied to a high degree of accuracy.

In figure 2*a* is shown a contour plot of the function $\partial N/\partial\tau$ in the case when $P = Q = 1$. It will be seen that the function has four positive maxima, all lying close to the characteristic directions $d\lambda = \pm\sqrt{2}d\mu$, as predicted in part I. The four positive maxima are separated by troughs of negative $\partial N/\partial\tau$ lying along the λ and μ -axes.

Figure 2*b* shows the 'frequency spectrum' $N(\omega)$ and the corresponding rate of change, $\partial N(\omega)/\partial\tau$. These are found by integrating N and $\partial N/\partial\tau$ along lines $\sigma = \text{constant}$, which are parallel to the μ -axis, in this approximation. The curve for $\partial N/\partial\tau$ shows a strongly negative minimum at the origin, with two positive maxima, symmetrically situated to either side.

The regions of negative energy transfer in figure 2*a* may be interpreted in the following way. We saw in part I, §3 that for resonant interactions to take place the four wavenumbers $\kappa_1, \kappa_2, \kappa_3, \kappa_4$ must lie at the corners of a parallelogram, with κ_1, κ_2 at opposite corners. Also they must all lie on a hyperbola with asymptotes parallel to the directions $d\lambda = \pm\sqrt{2}d\mu$. In §5 of part I it was pointed out that one such possibility was when κ_3 and κ_4 lay inside the peak, and κ_1, κ_2 outside the peak zone but in the characteristic directions as seen from the peak. This makes the terms $(N_1 + N_2)N_3N_4$ in the integrand larger in general than the terms $(N_3 + N_4)N_1N_2$, so the energy transfer to κ_1 is then *positive*.

However, a second possible configuration is when κ_2 and κ_4 lie inside the peak, and κ_1 and κ_3 outside it but near the directions of the λ - and μ -axes (see figure 3).

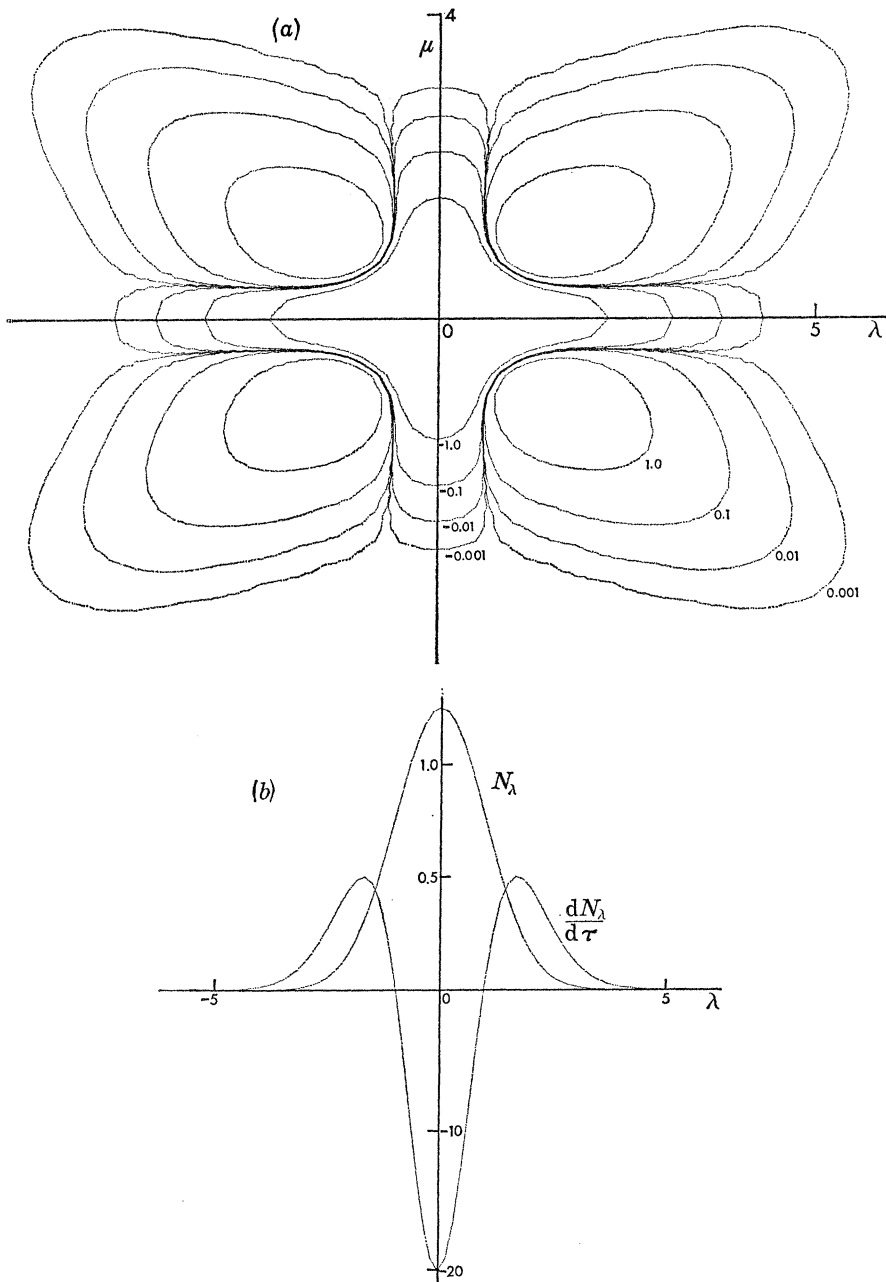


FIGURE 2. (a) Contours of the transfer function $\partial N/\partial \tau$ in the κ -plane, when the wave spectrum has the symmetrical normal form (3.1), in which $P = Q = 1$; $R = \sqrt{(2/PQ)}$. (b) The μ -integrated spectrum N_λ and transfer function $dN_\lambda/d\tau$ corresponding to figure 2a.

Then the largest terms in the integrand are

$$N_2 N_4 (N_3 - N_1). \tag{4.2}$$

But if κ_1 lies on the λ -axis, as in figure 3, then initially $(N_3 - N_1) < 0$ in general. Hence the energy transfer $\partial N / \partial \tau$ can be expected to be small but negative

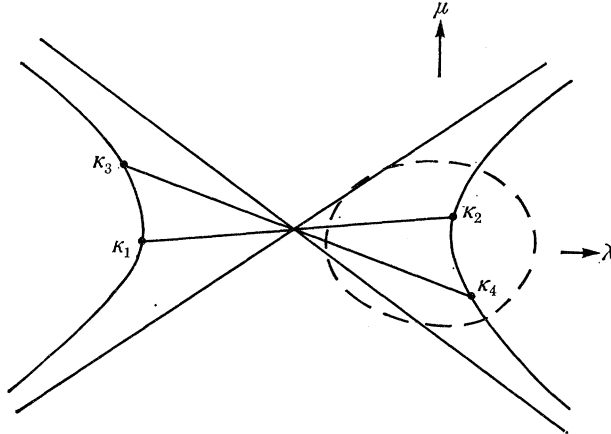


FIGURE 3. Four interacting wavenumbers, $\kappa_1, \kappa_2, \kappa_3, \kappa_4$, in the situation when κ_1 lies on the λ -axis and well outside the main peak.

5. ASYMMETRIC SPECTRA

The above method of calculation can be extended to narrow wave spectra consisting of the sum of two or more normal distributions:

$$N(\kappa) = R \sum_p a_p \exp \left[-\frac{1}{2} P_p (\lambda - \lambda_p)^2 - Q_p \mu^2 \right], \tag{5.1}$$

where a_p, P_p, Q_p, λ_p are arbitrary constants ($a_p, P_p, Q_p > 0$). Substitution into equation (3.2) then gives

$$\begin{aligned} \frac{\partial N}{\partial \tau} = & 4\pi R^3 \sum_p \sum_q \sum_r a_p a_q a_r \iiint \exp \left[-\frac{1}{2} \{ P_p (\lambda - \lambda_p)^2 + P_q (\lambda + \lambda' - \lambda'' - \lambda_q)^2 \right. \\ & \left. + P_r (\lambda + \lambda' + \lambda'' - \lambda_r)^2 \} - \{ Q_p \mu^2 + Q_q (\mu + \mu' - \mu'')^2 + Q_r (\mu + \mu' + \mu'')^2 \} \right] \frac{d\alpha d\beta' d\beta''}{|\beta' \beta''|} \\ & + \text{similar expressions.} \end{aligned} \tag{5.2}$$

Each of these terms may be treated in exactly the same way as before, although the final transformation from $\int_{-\frac{1}{2}\pi}^{\frac{1}{2}\pi} d\theta$ to $\int_0^{\frac{1}{2}\pi} d\theta$ requires the interchange of (p, q, r) and (p, r, q) in the sum (5.2).

By this method it is possible to estimate some of the effects of asymmetry in narrow spectra. In the following examples all spectra have been normalized so as to have a total (non-dimensional) action of π , that is, we have taken

$$R = \left[\sum_p a_n \sqrt{(2/P_n Q_n)} \right]^{-1}. \tag{5.3}$$

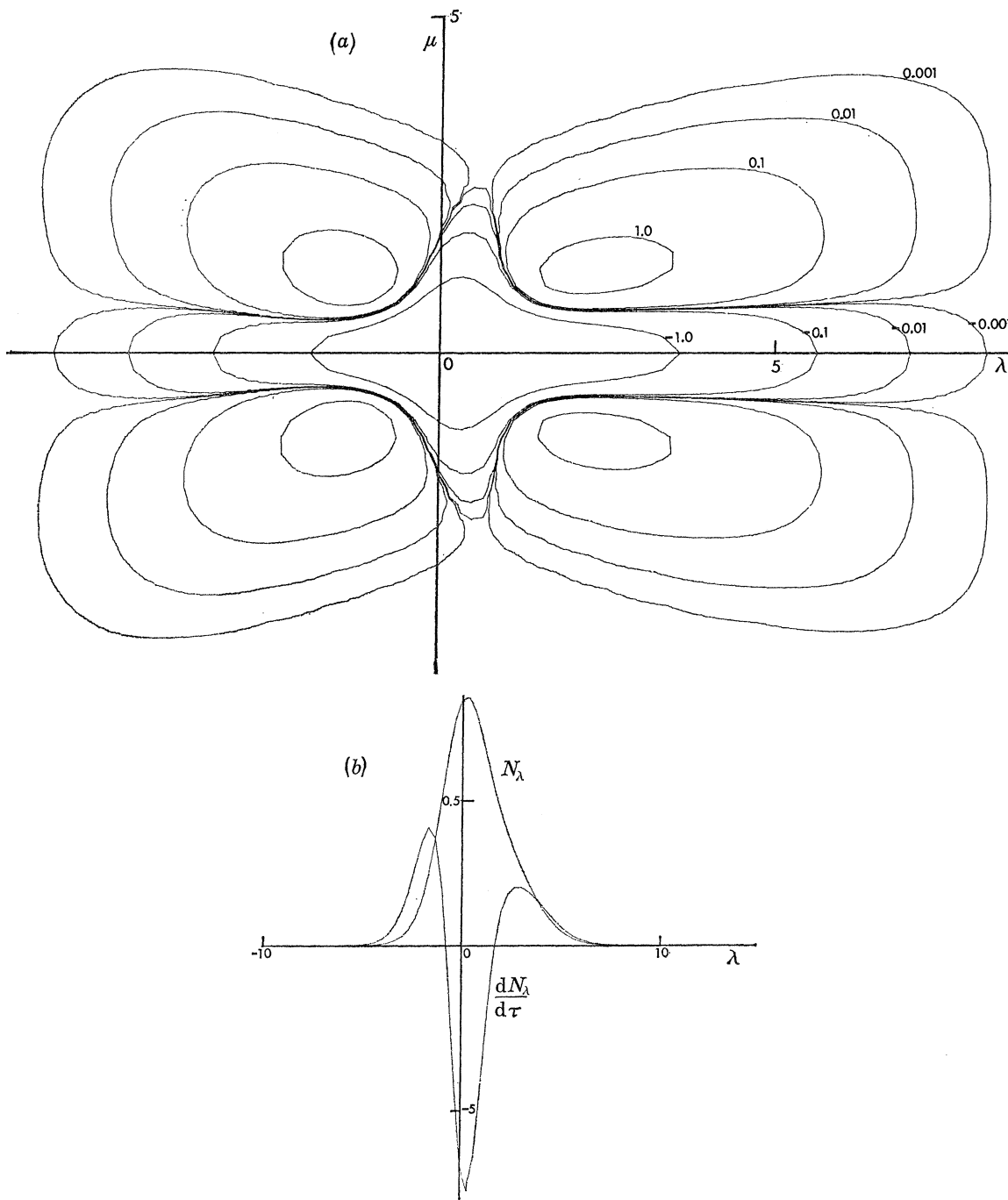


FIGURE 4. (a) Contours of the transfer function $\partial N/\partial \tau$ for the asymmetric spectrum given by (5.1), in which $P_1 = Q_1 = 1$; $P_2 = 0.3$, $Q_2 = 1$; $a_2/a_1 = 0.8$; $\lambda_1 = 0$, $\lambda_2 = 1.25$. (b) The μ -integrated spectrum N_λ and transfer function $dN_\lambda/d\tau$ corresponding to figure 4a.

Figures 4*a* and 4*b* show the results, comparable to figures 2*a* and 2*b*, for an initial spectrum consisting of two normal spectra having the same width in the μ -direction ($Q_1 = Q_2 = 1.0$) but different widths ($P_1 = 1.0, P_2 = 0.3$) in the λ -direction. The ratio of the amplitudes is 0.8, and the distance between centres is 1.25. In figure 4*a* the effect of this amount of asymmetry appears slight, but in figure 4*b* it can be seen that the μ -integrated transfer is markedly greater on the forward

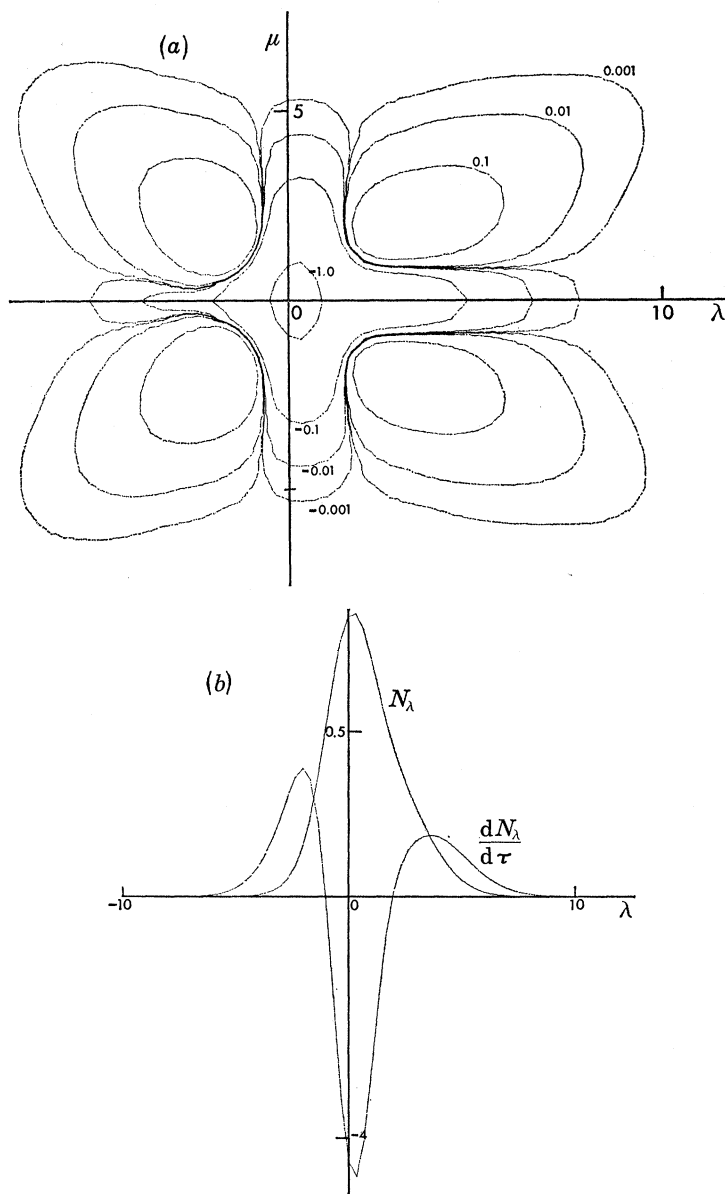


FIGURE 5. (a) As in figure 4*a*, but with $Q_1 = Q_2 = 0.25$. (b) The μ -integrated spectrum and transfer function corresponding to figure 5*a*.

(low-frequency) face of the spectrum. At the peak of the spectrum the transfer is still strongly negative.

In figures 5*a*, 5*b* and 6*a*, 6*b* the spectra have the same structure in the λ -direction as in figures 4*a*, 4*b*, but are successively broader in the μ -direction. Thus in figures 5*a*, 5*b*, $Q_1 = Q_2 = 0.25$ and in figures 6*a*, 6*b*, $Q_1 = Q_2 = 0.1$. The main effect can be seen in figures 5*a* and 6*a*, where the regions of negative transfer on the negative λ -axis are diminished in size and eventually become positive; whereas on the positive λ -axis the negative regions become comparatively deeper.

This can be attributed to the fact that in a spectrum which is broadened in the μ -direction the *positive* energy transfer described above tends to spread away from the asymptotes and onto the axes. But this transfer is proportional to $(N_1 + N_2) N_3 N_4$ and as κ_1 and κ_2 , are on *opposite* sides of the peak the positive transfer is relatively greater on the steeper (low-frequency) side, (tending to even out the asymmetry in the λ -direction). Hence it is on the steeper side that the negative transfer becomes blotted out.

6. A COMPARISON WITH NORTH SEA SPECTRA

Hasselmann *et al.* (1973) have presented numerical estimates of the weak non-linear energy transfer in spectra corresponding to wave observations in the North Sea (JONSWAP 1). Further details of the computations are given by Sell & Hasselmann (1972). The authors found that although for fairly broad spectra the energy transfer near the spectral peak was generally positive, nevertheless as the

TABLE 1. PARAMETERS CORRESPONDING TO THE SPECTRUM OF FIGURE 7

p	P_p	Q_p	a_p	λ_p
1	1.00000	0.03	1.000	0.000
2	0.08000	0.03	0.200	2.000
3	0.01563	0.03	0.625	7.656

TABLE 2. PARAMETERS CORRESPONDING TO THE SPECTRUM OF FIGURE 8

p	P_p	Q_p	a_p	λ_p
1	1.00000	0.03	1.000	0.000
2	0.08000	0.03	0.110	2.000
3	0.01563	0.03	0.045	7.656

peak was narrowed, this effect was diminished and even reversed in sign. Instead, the dominant effect was to shift the peak towards lower frequencies. The authors also suggested that the form of the wave spectrum, and the peak in particular, might be determined predominantly by the nonlinear energy transfer.

As noted earlier, however, Sell & Hasselmann (1972) were not able to compute the transfer function $\partial N / \partial \tau$ in any detail, because their computed results were not either stable enough or smooth enough to enable them to draw reliable contours of energy transfer in the wavenumber plane.

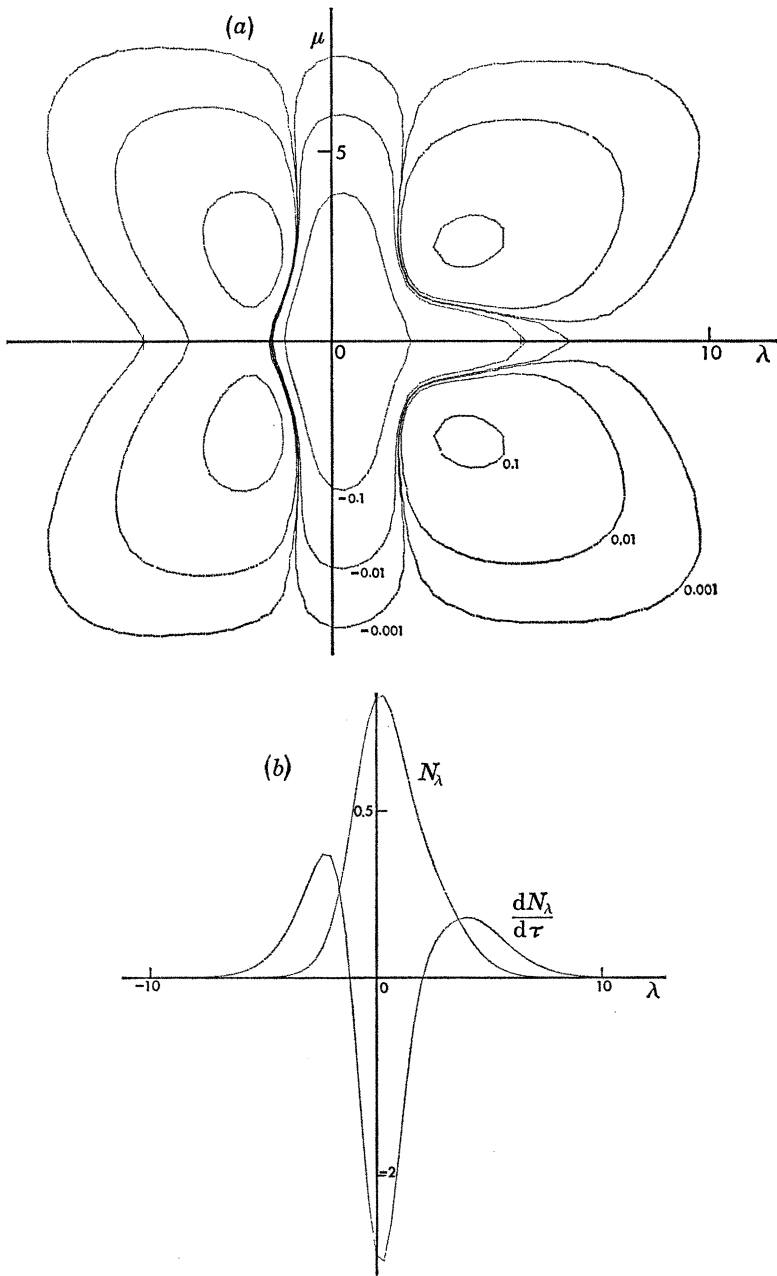


FIGURE 6. (a) As in figure 4a, but with $Q_1 = Q_2 = 0.25$. (b) The μ -integrated spectrum and transfer function corresponding to figure 6a.

Following the present method, we may compute the energy transfer given by equation (2.1) for an asymmetric spectrum having parameters chosen so as to approximate the observed wave spectra studied by Sell & Hasselmann.

Figure 7a shows a comparison between the 'mean JONSWAP spectrum' JN5 of Sell & Hasselmann (1972) and a spectrum consisting of the sum of three normal distributions as in equation (5.1). The values of the parameters are given in table 1

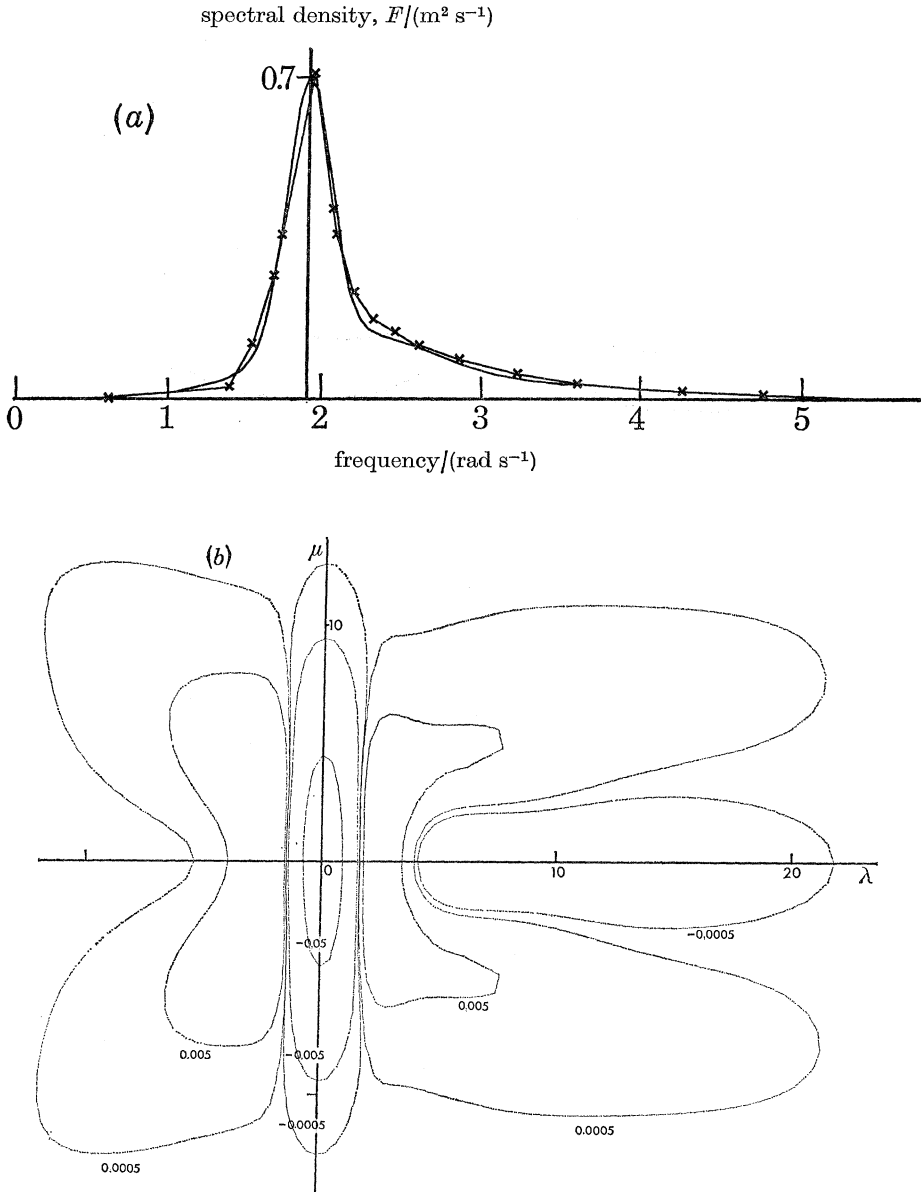


FIGURE 7. For description see opposite.

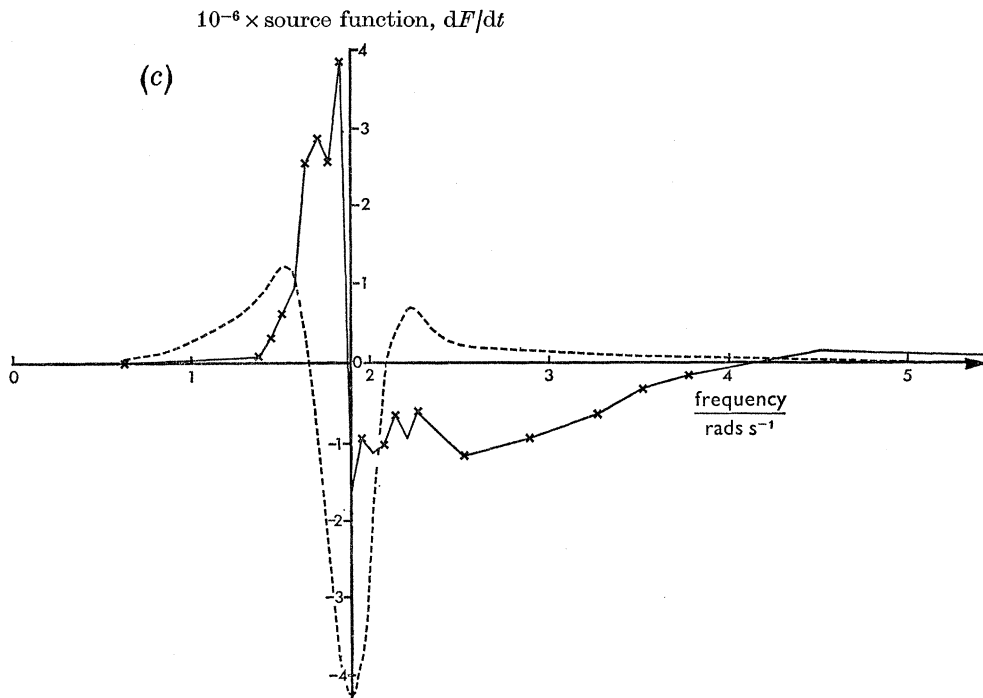


FIGURE 7. (a) The frequency spectrum corresponding to equation (5.1) (—) and the JONSWAP spectrum JN5 (\times — \times). (b) The computed transfer function $\partial N/\partial \tau$ corresponding to the spectrum of equation (2.1). (c) The μ -integrated transfer function for figure 7b, (---), compared with the numerical computations for JN5 by Sell & Hasselmann (1972) (\times — \times).

(for further details see appendix A). In figure 7b are shown the contours of the transfer function $\partial N/\partial \tau$ corresponding to equation (2.1). It will be seen that the transfer is rather similar to that in figure 6a, having four positive maxima, but being negative along the μ -axis and on certain parts of the positive λ -axis.

The μ -integrated transfer function is shown in figure 7c, converted to physical units (see appendix). For comparison we show the results of Sell & Hasselmann (with the frequency scale converted from Hz to rad/s). The curves agree as regards order of magnitude, and in the position of the minimum (i.e. maximum negative) transfer beneath the peak. However, the curve of Sell & Hasselmann is markedly less symmetrical. This must be attributed mainly to the asymmetry of the (8-dimensional) coupling coefficient $G(\kappa_1, \kappa_2, \kappa_3, \kappa_4)$ which in our approximation is a constant.

Corresponding results for the 'sharp JONSWAP spectrum' R3C are shown in figures 8a, b and c. The parameters in this case are given in table 2. From figure 8c we see that the agreement between the computed transfer functions is now much closer, both the central minimum and the two side maxima being reproduced fairly well. No doubt this is due to the fact that the spectrum is narrower and the

narrow-band approximation correspondingly better. It should be noted that in the computations of Sell & Hasselmann, greater resolution is really required to determine both the position of the central minimum, and the transition from positive to negative transfer on the left of the peak. This transition will affect the rate at which the peak energy is displaced towards lower frequencies.

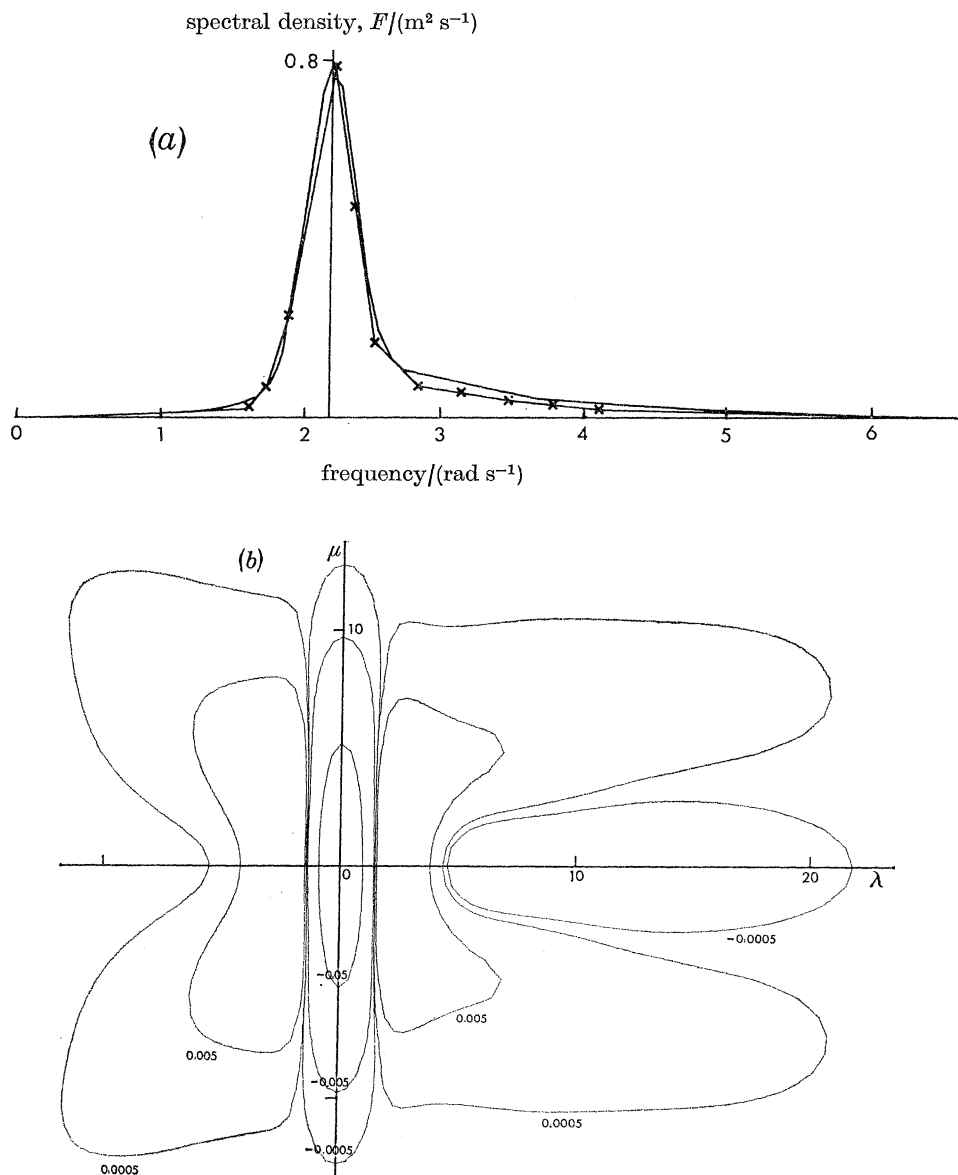


FIGURE 8. For description see opposite.

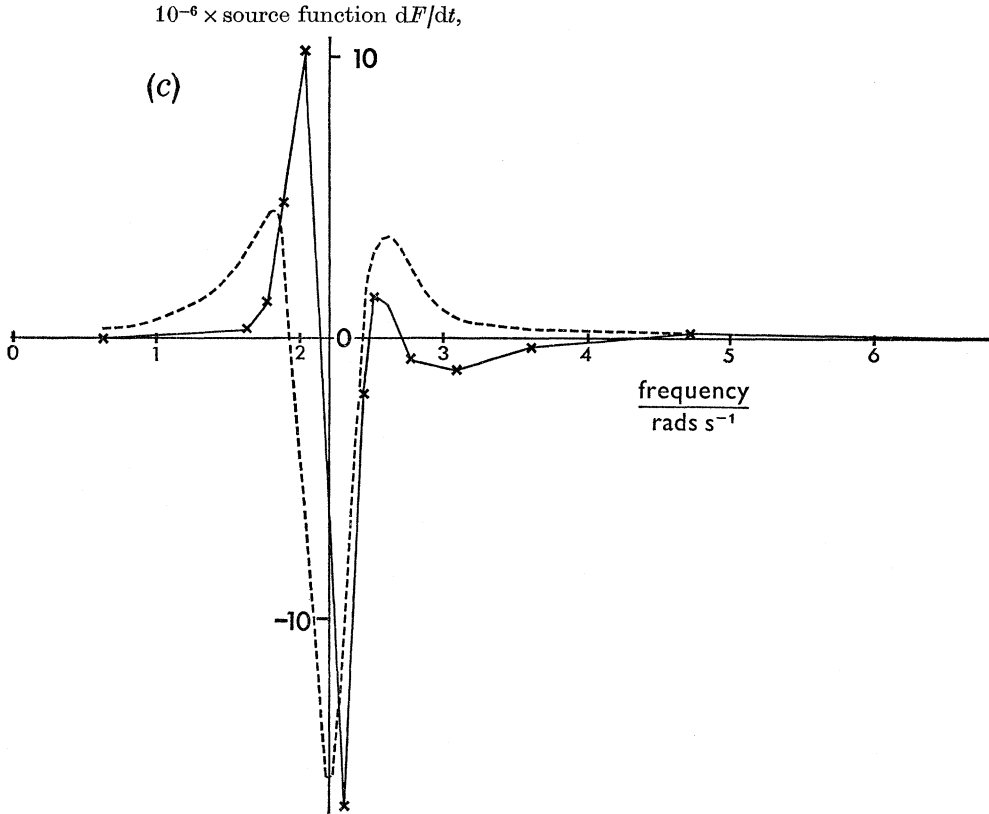


FIGURE 8. (a) The frequency spectrum corresponding to equation (5.1) (—) and the JON-SWAP spectrum R3C ($\times - \times$). (b) The computed transfer function $\partial N/\partial \tau$ corresponding to the spectrum of equation (5.1). (c) The μ -integrated transfer function for figure 8b, (---) compared with the numerical computations for R3C by Sell & Hasselmann (1972) ($\times - \times$).

7. FURTHER DISCUSSION

From equation (2.1) it can be seen that, for spectra of the same shape, $\partial N/\partial \tau$ is proportional to $A^3 L^2$ where A is a scale for the amplitude and L a scale in the (λ, μ) -plane. Hence the μ -integrated transfer rate is proportional to $A^3 L^3$. But the amplitude B of the μ -integrated spectrum F is proportional to AL . Hence

$$\partial F/\partial \tau = SB^3,$$

where S is a function of the spectral shape alone. Table 3 shows the computed values of S when for A we take the peak spectral density and for B the value of the μ -integrated spectrum at the negative peak of the transfer function.

In table 3, the two spectra which are broadest in the μ -direction are the last two, cases 5 and 6. Thus there appears a general tendency for the transfer function of a given frequency spectrum to diminish as the corresponding angular spread increases.

TABLE 3. SCALE FACTORS FOR CERTAIN SPECTRA

case	A	B	S	comments
1	1.3	20.0	9.1	symmetric spectrum, see §4
2	0.8	7.5	14.7	} asymmetric spectra with the same λ-dependence, successively broader in the μ -direction, see §5
3	0.8	4.7	9.28	
4	0.8	2.9	5.7	
5	0.7	0.9	2.6	
6	0.8	1.2	2.3	similar to JONSWAP JN5 similar to JONSWAP R3C

8. CONCLUSIONS

By adopting a certain analytic description of the energy spectrum (equation (5.1)) we have been able to reduce the energy transfer integral to a manageable form, and hence, for a sufficiently narrow spectrum, to compute the energy transfer precisely. It turns out that the maximum energy transfer does indeed lie close to the characteristic directions predicted earlier, with minima, or 'valleys' lying along the axes of symmetry.

For the 'sharp JONSWAP spectrum' we find that the integrated transfer function agrees well with the rough computations of Sell & Hasselmann (1972), for which the transfer becomes more symmetric as the spectrum is narrowed. For even narrower spectra the transfer will presumably be still more symmetric, and the negative maximum at the peak will be enhanced.

Our results suggest always a tendency for the spectral peak to become broader. There is no indication that a peak could be built up by the weak nonlinear energy transfer. Presumably the building up of narrow spectra requires the continuing accompaniment of energy input from the wind.

I am indebted to Professor M. S. Longuet-Higgins, F.R.S., for suggesting this problem, and for his guidance in the preparation of this paper. I am indebted also to the Natural Environment Research Council for the support of a research studentship.

APPENDIX. COMPARISONS WITH FIELD DATA

For a comparison with the JONSWAP spectrum JN5 of Sell & Hasselmann (1972)† we have the following parameters

$$\text{frequency at peak: } \sigma_p = 0.3 \text{ Hz} = 0.6 \pi \text{ s}^{-1},$$

width of peak at half

$$\text{maximum intensity: } \sigma_w = 0.053 \text{ Hz} = 0.106 \pi \text{ s}^{-1},$$

$$\text{height of peak: } N_p = 0.24 \text{ m}^2/\text{Hz} = 0.12 \pi^{-1} \text{ m}^2 \text{ s}.$$

We must transform to nondimensional units in which $g = 1$, $\sigma_p = 1$. This gives

† This is equivalent to the spectrum shown in figure 2.21 (c) of Hasselmann *et al.* 1973, but is *not* the same as figure 2.12 of that paper, in which the spectrum has been rescaled.

$\sigma_w = 0.053/0.3 = 0.177$ and $N_p = (0.6 \pi)^5 / (9.8)^2 \times 0.12 \pi^{-1}$. We must also transform from units of (frequency) $^{-1}$ to units of (wavenumber) $^{-1}$. Since from §2 of part I,

$$\sigma = \frac{1}{2}\epsilon\lambda + \epsilon^2\omega + O(\epsilon^3)$$

we have the lowest order in ϵ .

width of peak in

wavenumber space: $\lambda_w = (2/\epsilon) \times 0.177,$

energy spectrum: $E(\sigma) = \epsilon^2\sigma F(\sigma) \simeq \epsilon^2 F(\sigma),$

with $F(\sigma) d\sigma = F(\lambda) d\lambda$. Hence the height of the peak in wavenumber space is

$$N_\lambda = N_p \times \frac{1}{2\epsilon}.$$

In the JONSWAP spectrum an angular spreading factor proportional to $\cos^2\theta$ was assumed. Hence the width of the peak in the m -direction was $\frac{3}{2}$ times the wavenumber of the peak in the l -direction, giving $\mu_w = 1.5\epsilon^{-1}$, so $\mu_w/\lambda_w \simeq 4.0$. Accordingly in the spectrum of figure 7 we have taken for the largest term in the sum: $P_1 = 1.0$, $Q_1 = 0.03$, so $\frac{1}{2}P_1/Q = 16.0 \simeq (\mu_w/\lambda_w)^2$. These and the remaining parameters of the spectrum in figure 7a are given in table 1.

For comparison of the μ -integrated spectrum $F(\lambda)$ with, say, the JONSWAP spectrum JN5, the scale of N must be multiplied by

$$(N_p/A) \sigma_p^5 / (2\epsilon g^2)$$

and the scale of the integrated transfer rate $\partial F/\partial\tau$ must be multiplied by the cube of this factor. Converting now to the frequency spectrum, we must multiply by a further factor $(2/\epsilon)$. Since also $E = \epsilon^2\sigma_p N$ and $t = \epsilon^{-2}\tau$ we have

$$\frac{\partial E}{\partial t} = \epsilon^4\sigma_p \frac{\partial N}{\partial \tau}.$$

Lastly, to express the result in units of m^2 we must multiply by g^2/σ_p^2 , giving altogether a scale factor

$$\frac{1}{4}(N_p/A)^3 \sigma_p^{11}/g^4 = 4.7 \times 10^{-6} m^2$$

for JN5 and case 5. This is used in figure 7c.

For the R3C spectrum the appropriate parameters are $\sigma_p = 0.35$ Hz, $\sigma_w = 0.067$ Hz and $N_p = 0.22 m^2/\text{Hz}$. Converting these to the appropriate units we have for case 6 a corresponding scale factor $1.3 \times 10^{-5} m^2$. This is used in figure 8c.

REFERENCES

Davey, A. & Stewartson, K. 1974 On three-dimensional packets of surface waves. *Proc. R. Soc. Lond. A* **338**, 101–110.
 Hasselmann, K. *et XV al.* 1973 Measurements of wind-wave growth and swell decay during the joint North Sea wave project. *Erganzungsheft zur Deutsch. Hydrogr. Z.* A **12**, 95 pp.
 Longuet-Higgins, M. S. 1975 On the nonlinear transfer of energy in the peak of a gravity-wave spectrum. *Proc. R. Soc. Lond. A* **347**, 311.
 Sell, W. & Hasselmann, K. 1972 Computations of nonlinear energy transfer for JONSWAP and empirical wind-wave spectra. *Rep. Inst. Geophys., Univ. Hamburg.*